DNAPKcs-dependent arrest of RNA polymerase II transcription in the presence of DNA breaks

Tibor Pankotai[1], Céline Bonhomme[1], David Chen[2] & Evi Soutoglou[1]

DNA double-strand break (DSB) repair interferes with ongoing cellular processes, including replication and transcription. Although the process of replication stalling upon collision of replication forks with damaged DNA has been extensively studied, the fate of elongating RNA polymerase II (RNAPII) that encounters a DSB is not well understood. We show that the occurrence of a single DSB at a human RNAPII-transcribed gene leads to inhibition of transcription elongation and reinitiation. Upon inhibition of DNA protein kinase (DNAPK), RNAPII bypasses the break and continues transcription elongation, suggesting that it is not the break per se that inhibits the processivity of RNAPII, but the activity of DNAPK. We also show that the mechanism of DNAPK-mediated transcription inhibition involves the proteasome-dependent pathway. The results point to the pivotal role of DNAPK activity in the eviction of RNAPII from DNA upon encountering a DNA lesion.

DNA lesions endanger cell viability by affecting fundamental DNA-dependent nuclear processes such as replication and transcription[1–3]. During the S phase of the cell cycle, collision of replication forks with damaged DNA stalls ongoing DNA replication[3]. Moreover, RNA polymerases are stalled at bulky lesions and are subsequently removed, by ubiquitination and proteasome dependent degradation in transcription-coupled repair[4–6]. Recent studies have shown that RNAPI and RNAPII transcription machineries are affected by the presence of DSBs and that transcription is transiently repressed[7–9]. DSBs upstream of the promoter of an RNAPII reporter gene inhibited transcription elongation due to ataxia telangiectasia mutated (ATM)-dependent signaling and the spreading of ubiquitination[7]. Similarly, DNA break–dependent RNAPI inhibition was mediated by the ATM kinase activity[8]. In addition, Poly(ADP-ribose) polymerase 1 (PARP1) was shown to have a role in removing nascent RNA and elongating RNAPII from sites of DNA damage induced by microirradiation, suggesting that under conditions where a variety of lesions are induced, PARP1 sets up a repressive chromatin structure to block transcription by recruiting members of the polycomb complex[10]. Although there is increasing evidence of interplay between transcription and DNA repair, the dynamics of the RNAPII machinery upon encountering a single DSB during transcriptional elongation have not been addressed.

To address this question, we took advantage of the site-specific meganuclease I-PpoI that has several recognition sequences in the human genome and was previously used to induce single DSBs in human cells at defined positions[11]. We used this system to examine how the presence of a DSB, and the mounting of the subsequent DNA damage response (DDR), affect the transcriptional output of genes harboring I-PpoI recognition sequences. Using this system, we show that induction of a single DSB at an RNAPII-transcribed gene leads to DNAPK-dependent inhibition of transcription. DNAPK catalytic subunit (DNAPKcs) activity is required for evicting RNAPII from the DNA when a DNA lesion is encountered. We demonstrate that upon inhibition of DNAPK, RNAPII bypasses the break and continues transcription elongation. DNAPK-mediated silencing occurs through a mechanism that involves proteasome-dependent degradation. Our results suggest that DNAPK activity is required to prevent transcription through strand breaks, pointing to a previously unknown role for this kinase in preventing the production of mutated transcripts.

RESULTS

Double-strand breaks induce arrest of RNAPII transcription

To investigate the dynamics of RNAPII transcription machinery in the presence of DSBs, we took advantage of the I-PpoI endonuclease, which has natural cleavage sites in the human genome. In addition to the well-characterized target site for I-PpoI in the 28S ribosomal RNA gene and the recently characterized unique cleavage site in an intron of the *DAB1* gene on human chromosome 1 (ref. 11), we identified an additional 14 recognition sequences (**Supplementary Fig. 1a**) by using *in silico* analysis. To investigate RNAPII transcription kinetics following I-PpoI DNA break induction, we established stable HeLa and HEK293T cell lines expressing the I-PpoI enzyme, fused to the ligand-binding domain of the estrogen receptor (ER)[11]. Addition of 4-hydroxytamoxifen (4-OHT) to both stable cell lines resulted in a time-dependent nuclear translocation of I-PpoI and cleavage of the endogenous 28S rDNA I-PpoI site, as demonstrated by the induction of γ-H2AX, mainly around nucleoli (**Supplementary Fig. 1b**).

Figure 1 RNAPII transcription inhibition in response to DSBs. (**a**) Schematic representation of three RNAPII-transcribed genes that harbor an I-PpoI cleavage site. The position of the break (red arrow) and the primers for quantification of the mRNA (small black arrows) or DNA (small red arrows) content are indicated. (**b**) Quantitative PCR with reverse transcription (qRT-PCR) analysis of *DAB1*, *RYR2* and *INTS4* expression levels and cutting efficiencies in HeLa (top) and HEK293T (bottom) cells at different time points after the addition of 4-OHT. mRNA values are normalized to cyclophilin B. Values for DNA content are normalized to a part of the gene not affected by the break. Values represent mean ± s.d. from three independent experiments.

Among the five RNAPII-regulated genes that contain I-PpoI recognition sites, we chose to study *DAB1*, *RYR2* and *INTS4*, as they were adequately expressed in both HeLa and HEK293T cells (**Fig. 1a** and data not shown). Notably, the nuclear translocation of I-PpoI resulted in site-specific DNA breaks at *DAB1* and *RYR2* but not at *INTS4* (**Fig. 1a,b**). Sequencing of the *INTS4* gene revealed that the I-PpoI site was degenerate in HEK293T cells but not in HeLa cells (**Supplementary Fig. 1c**). We thought the absence of a DSB at the *INTS4* I-PpoI site in HeLa cells might be due to the structure of the surrounding chromatin that restricts the access of the endonuclease to the site. We thus used the *INTS4* gene throughout this study as a negative control. Transcription inhibition, demonstrated by the reduction of the mature and nascent RNA levels of *DAB1* and *RYR2*, was transient and concomitant with break induction (**Fig. 1b** and **Supplementary Fig. 2a**). Transcription restoration closely followed the dynamics of the repair of the breaks in both cell lines (**Fig. 1b** and **Supplementary Fig. 2a**): after 3–4 h, transcription levels increased, with full restoration occurring approximately 6 h following the initial break induction. Similarly, 3–4 h after the initiation of DSBs, we began to detect an increase in repaired I-PpoI sites, with completion of repair reaching a plateau at approximately 6 h (**Fig. 1b** and **Supplementary Fig. 2a**). As expected, the relative expression of *INTS4* and two other control genes (*ATAC2*, also known as *CSRP2BP*, and *B-ACTIN*, also known as *ACTB*), which do not have I-PpoI cleavage sites, were not altered (**Fig. 1b** and **Supplementary Fig. 2b**). These data suggest a specific inhibition of RNAPII transcription at I-PpoI targeted genes.
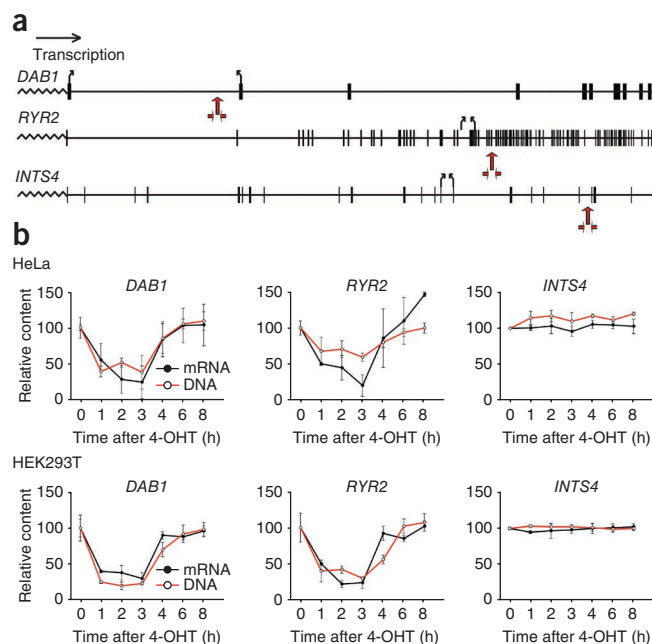
DSB-induced transcription inhibition depends on DNAPKcs

ATM and DNAPK bind at sites of DNA damage and are necessary for DDR and repair[12–15]. These two proteins are associated with DSBs in a different fashion: DNAPK is recruited near the broken ends, whereas ATM spreads from the DSB into very large domains of the surrounding chromatin[12–15]. To determine whether spreading of DDR signaling or a local event is involved in blocking RNAPII transcription in response to DSBs, we measured the relative mRNA levels of *DAB1* and *RYR2* genes in the presence of ATM and DNAPKcs inhibitors. Notably, inhibition of DNAPKcs but not ATM rescued the transcription arrest in both cell lines (**Fig. 2a** and **Supplementary Fig. 2c**). These results suggest that when the break occurs at a coding region of an RNAPII-transcribed gene, the ATM-dependent spreading of the DDR is not sufficient to induce break-dependent transcriptional arrest. In agreement with this, the induction of I-PpoI breaks did
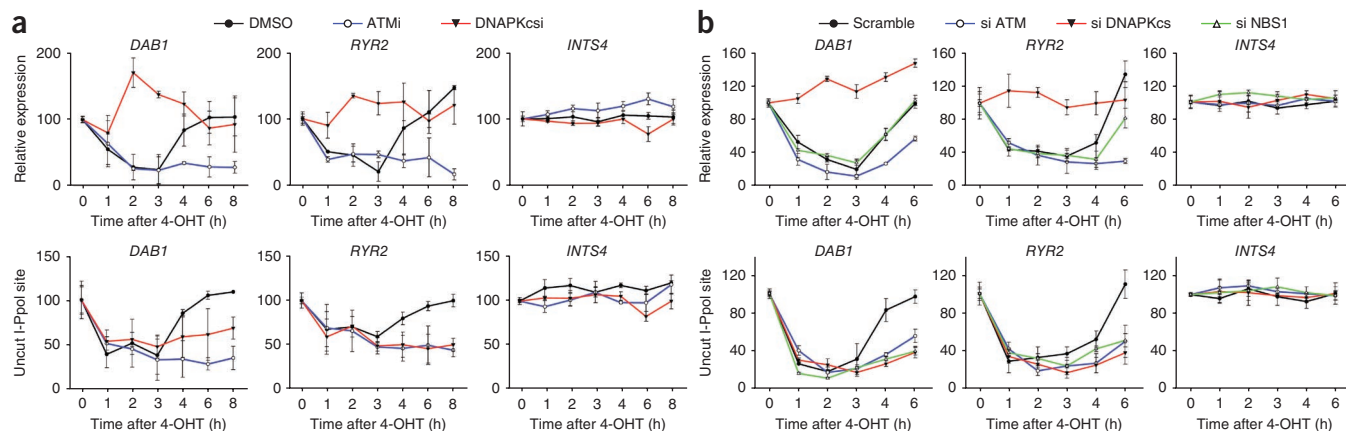
Figure 2 DNAPKcs-dependent transcriptional arrest after DSB induction. (**a**) qRT-PCR analysis of *DAB1*, *RYR2* and *INTS4* expression levels and cutting efficiency in HeLa cells treated with DMSO, ATM inhibitor (ATMi) and DNAPKcs inhibitor (DNAPKcsi) at different time points upon addition of 4-OHT. mRNA values (top) are normalized to cyclophilin B. Values for DNA content (bottom) are normalized to a part of the gene not affected by the break. Values represent mean ± s.d. from three independent experiments. (**b**) qRT-PCR analysis of *DAB1*, *RYR2* and *INTS4* expression levels and cutting efficiencies in HeLa cells treated with siRNA that targets a scramble sequence, the ATM sequence (si ATM), the DNAPKcs sequence (si DNAPKcs) and the NBS1 sequence (si NBS1) at different time points after the addition of 4-OHT. mRNA values (top) are normalized to cyclophilin B. Values for DNA content (bottom) are normalized to a part of the gene not affected by the break. Values represent mean ± s.d. from three independent experiments.
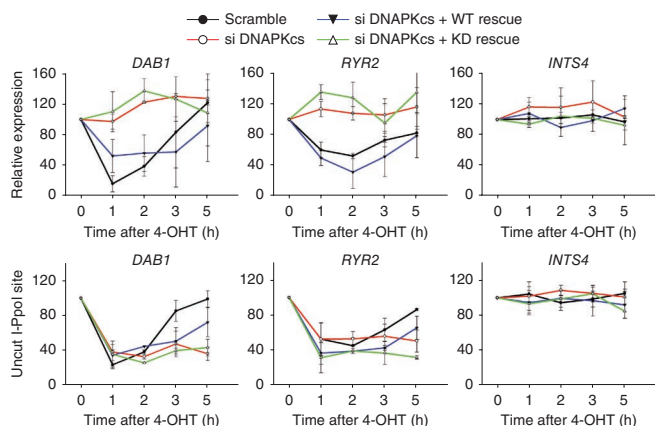
Figure 3 The essential role of DNAPKcs kinase activity in break-dependent transcriptional arrest. Quantification of *DAB1*, *RYR2* and *INTS4* expression levels and cutting efficiencies in HeLa cells treated with siRNA against a scramble sequence and against DNAPKcs (si DNAPKcs) and in cells treated with siRNA against DNAPKcs and complemented with wild-type (WT) or kinase-dead (KD) DNAPKcs. mRNA values (top) are normalized to cyclophilin B. Values for DNA content (bottom) are normalized to a part of the gene not affected by the break. Values represent mean ± s.d. from three independent experiments.

not affect the transcription of the genes adjacent to *DAB1* and *RYR2*, despite spreading of γ-H2AX to neighboring loci (**Supplementary Fig. 3a,b**). Our results are in agreement with a recent study, in which transcription and RNAPII association were accurately maintained within γ-H2AX domains[16]. As anticipated, inhibition of ATM and DNAPKcs resulted in delayed repair, illustrated by the reduced DNA content of *DAB1* and *RYR2* genes at 6 h following 4-OHT addition, compared to control (**Fig. 2a** and **Supplementary Fig. 2c**). To exclude the possibility that inhibition of DNAPKcs results in increased mRNA stability instead of transcription restoration, we quantified the relative levels of nascent RNA transcripts of *DAB1*, *RYR2* and *INTS4* under the different inhibitory conditions. DNAPKcs inhibition resulted in the reappearance of the nascent RNA transcripts of both *DAB1* and *RYR2* in HEK293T and HeLa cell lines, pointing to the rescue of transcription (**Supplementary Fig. 3c**).

Short interfering RNA (siRNA)-mediated silencing of DNAPKcs, ATM and NBS1, a DDR sensor responsible for the recruitment of ATM to breaks, recapitulated the effects observed by the inhibitors at the RNA and DNA levels of all three genes (**Fig. 2b** and **Supplementary Fig. 4a**). As expected, only the reduction of DNAPKcs rescued transcription in the presence of a DNA break (**Fig. 2b** and **Supplementary Fig. 4a**).

To further investigate the involvement of the kinase activity of DNAPKcs in transcriptional arrest, we complemented cells where endogenous DNAPKcs was knocked down by siRNA with plasmids that express siRNA-resistant forms of wild-type and kinase-deficient DNAPKcs (YFP-DNAPKcs K3753R)[17,18] (**Fig. 3** and **Supplementary Fig. 4b**). Complementation with wild-type DNAPKcs resulted in transcription inhibition, whereas addition of a kinase-deficient mutant of DNAPKcs did not revert the rescue phenotype (**Fig. 3** and **Supplementary Fig. 4b**), suggesting that the enzymatic activity is necessary for the transcriptional inhibition observed after the break.

DSB-induced transcription inhibition depends on Ku

DNAPKcs is recruited to DSBs by the DNA end–sensing complex Ku80–Ku70 (ref. 18). To test whether the function of DNAPKcs on

DSB-induced transcription arrest depends on the Ku heterodimer, we measured the relative mRNA levels of *DAB1* and *RYR2* in cells depleted of either Ku80 or Ku70 by siRNA. As expected, downregulation of Ku80 or Ku70 rescued transcription inhibition after 4-OHT treatment, which follows the pattern of DNAPKcs action (**Fig. 4** and **Supplementary Fig. 4c**). This observation supports the notion that the association of DNAPKcs with DSBs is essential for the transcriptional inhibition observed upon DSB occurrence and excludes the possibility of an indirect effect. To investigate whether other components of the nonhomologous end-joining repair pathway, such as XRCC4 or ligase IV, that act downstream of DNAPKcs[19] exert similar effects, we depleted XRCC4 and ligase IV using siRNA. We observed that XRCC4 and ligase IV did not contribute to the effect exerted by inhibition of DNAPKcs (**Fig. 4** and **Supplementary Fig. 4c**). Taken together, these results demonstrate that the NHEJ proteins that act upstream but not downstream of DNAPKcs in breaks rescue the DSB-mediated transcriptional inhibition. Moreover, it has been previously shown that depletion of XRCC4 results in a stronger association of DNAPKcs with DNA breaks[18], further supporting the necessity of DNAPKcs binding to breaks associated with transcription inhibition. As expected, depletion of XRCC4 and ligase IV resulted in a delay of repair, as judged by the decreased DNA content of both *DAB1* and *RYR2* genes after the induction of the break by I-PpoI (**Fig. 4** and **Supplementary Fig. 4c**).

The downregulation of the target genes by siRNA as well as the rescue of the endogenous DNAPKcs levels after re-expression of siRNA-resistant wild-type and kinase-dead forms of DNAPKcs was confirmed by western blot (**Supplementary Fig. 5a,b**). Moreover, we confirmed that re-expression of siRNA-resistant wild-type, but not the kinase-dead, form of DNAPKcs rescues the capacity of DNAPKcs for autophosphorylation at Ser2056 (**Supplementary Fig. 5c**).

DSB at gene body affects RNAPII elongation and reinitiation

To gain insight into the mechanism of transcriptional arrest that occurs after DSB induction, we monitored elongating and initiating RNAPII by chromatin immunoprecipitation (ChIP), using two different antibodies that recognize all forms of RNAPII and are
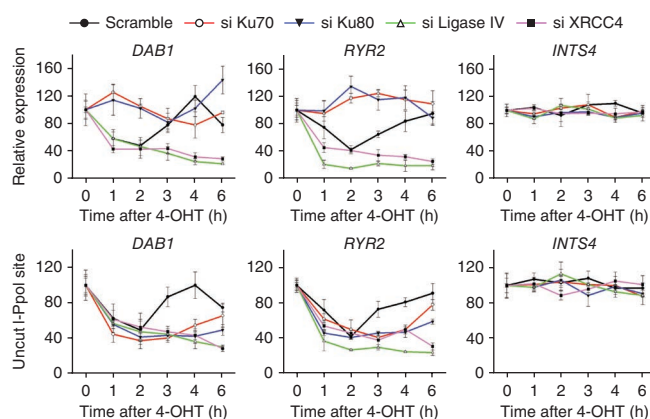

Figure 4 The Ku80–Ku70 complex is involved in transcriptional inhibition after DSB induction. qRT-PCR analysis of *DAB1*, *RYR2* and *INTS4* expression levels and cutting efficiencies in HeLa cells treated with siRNA that targets a scramble sequence, the Ku70 sequence (si Ku70), the Ku80 sequence (si Ku80), the ligase IV sequence (si Ligase IV) and the XRCC4 sequence (si XRCC4) at different time points after the addition of 4-OHT. mRNA values (top) are normalized to cyclophilin B. Values for DNA contents (bottom) are normalized to a part of the gene not affected by the break. Values represent mean ± s.d. from three independent experiments.

insensitive to phosphatase treatment (**Fig. 5** and **Supplementary Figs. 6** and **7**). At the same time, we confirmed DSB induction by I-PpoI using ChIP against γ-H2AX (**Fig. 5** and **Supplementary Fig. 7**). I-PpoI break induction led to displacement of RNAPII from the gene body and promoter of *DAB1* and *RYR2* genes (**Fig. 5a,b** and **Supplementary Figs. 6a** and **7a,b**). These results suggest that DSBs at an RNAPII-transcribed gene affect both the elongation and the initiation of transcription, in line with the suggestion that RNAPII transcription elongation and initiation are interlinked[20,21]. As expected, inhibition of ATM activity had a more marked effect on

RNAPII displacement and delayed restoration of RNAPII occupancy, correlating with delayed repair (**Fig. 5a,b** and **Supplementary Figs. 6a** and **7a,b**).

Notably however, when the DNAPKcs activity was inhibited, RNAPII remained associated with the promoter and the body of *DAB1* and *RYR2* genes (**Fig. 5a,b** and **Supplementary Figs. 6a** and **7a,b**). We observed comparable RNAPII occupancy at the gene bodies before and after the I-PpoI–induced breaks, demonstrating that in the absence of DNAPKcs, RNAPII can circumvent the break. Thus, the activity of DNAPKcs and not the break itself causes
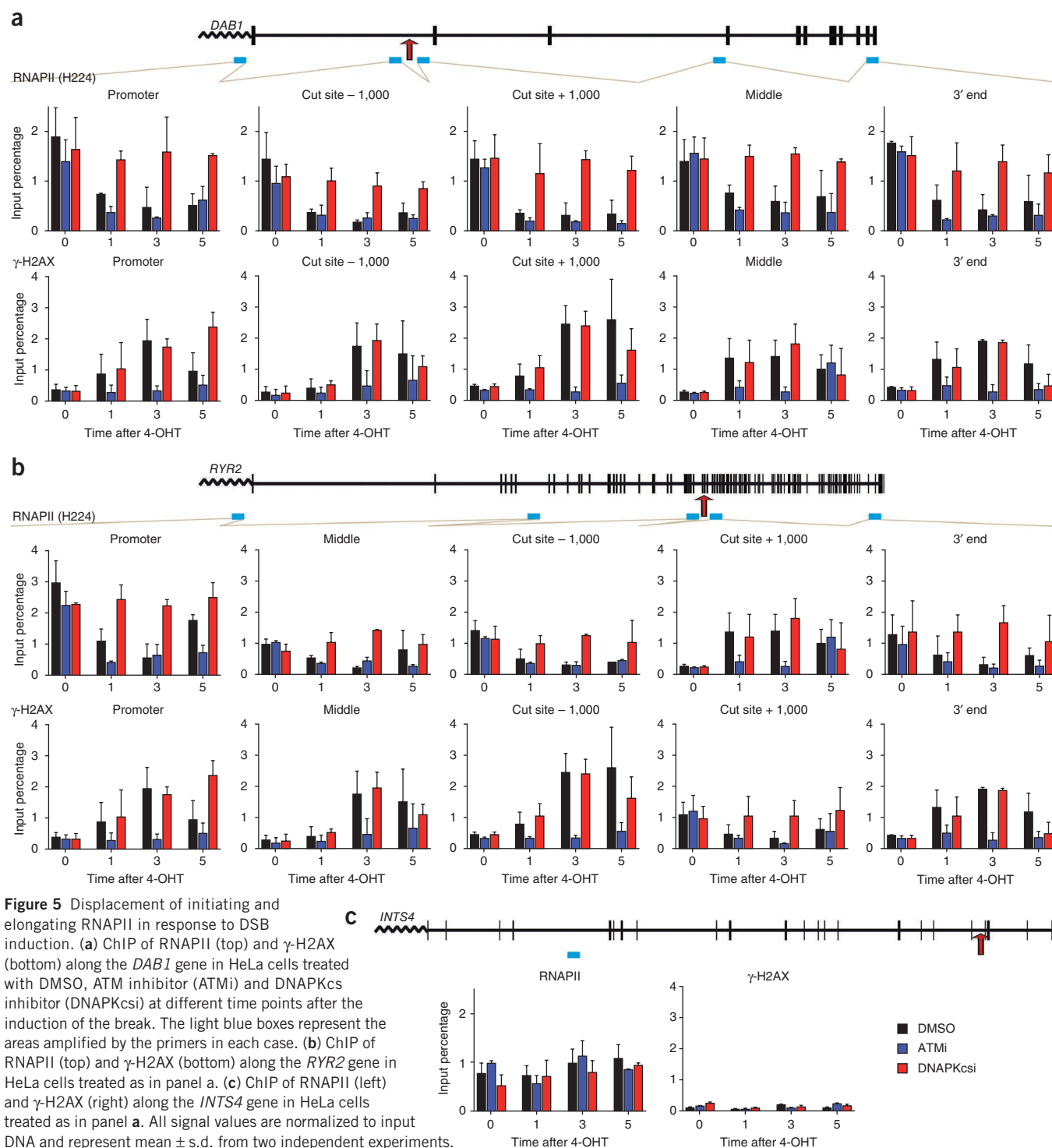
Figure 5 Displacement of initiating and elongating RNAPII in response to DSB induction. (**a**) ChIP of RNAPII (top) and γ-H2AX (bottom) along the *DAB1* gene in HeLa cells treated with DMSO, ATM inhibitor (ATMi) and DNAPKcs inhibitor (DNAPKcsi) at different time points after the induction of the break. The light blue boxes represent the areas amplified by the primers in each case. (**b**) ChIP of RNAPII (top) and γ-H2AX (bottom) along the *RYR2* gene in HeLa cells treated as in panel a. (**c**) ChIP of RNAPII (left) and γ-H2AX (right) along the *INTS4* gene in HeLa cells treated as in panel **a**. All signal values are normalized to input DNA and represent mean ± s.d. from two independent experiments.

Figure 6 RNAPII travels on the damaged DNA and overcomes the break. (**a**) Sequential ChIP of RNAPII and γ-H2AX along the *DAB1* (upper panel) and *RYR2* (lower panel) genes in HEK293T cells treated with DMSO, ATM inhibitor (ATMi) and DNAPKcs inhibitor (DNAPKcsi) at 0 h, 1 h, 3 h and 5 h after the addition of 4-OHT. Signal values are normalized to input DNA. Values represent mean ± s.d. from the three PCR replicates of one representative experiment. (**b**) Quantification of nascent RNA levels of *DAB1*, *RYR2* and *INTS4* in HeLa cells treated with DMSO, ATM inhibitor and DNAPKcs inhibitor, at 0–4 h after addition of 4-OHT. The sequence amplified corresponds to the part of the transcript that is produced after the I-Ppol cleavage site. Values represent mean ± s.d. from three independent experiments.
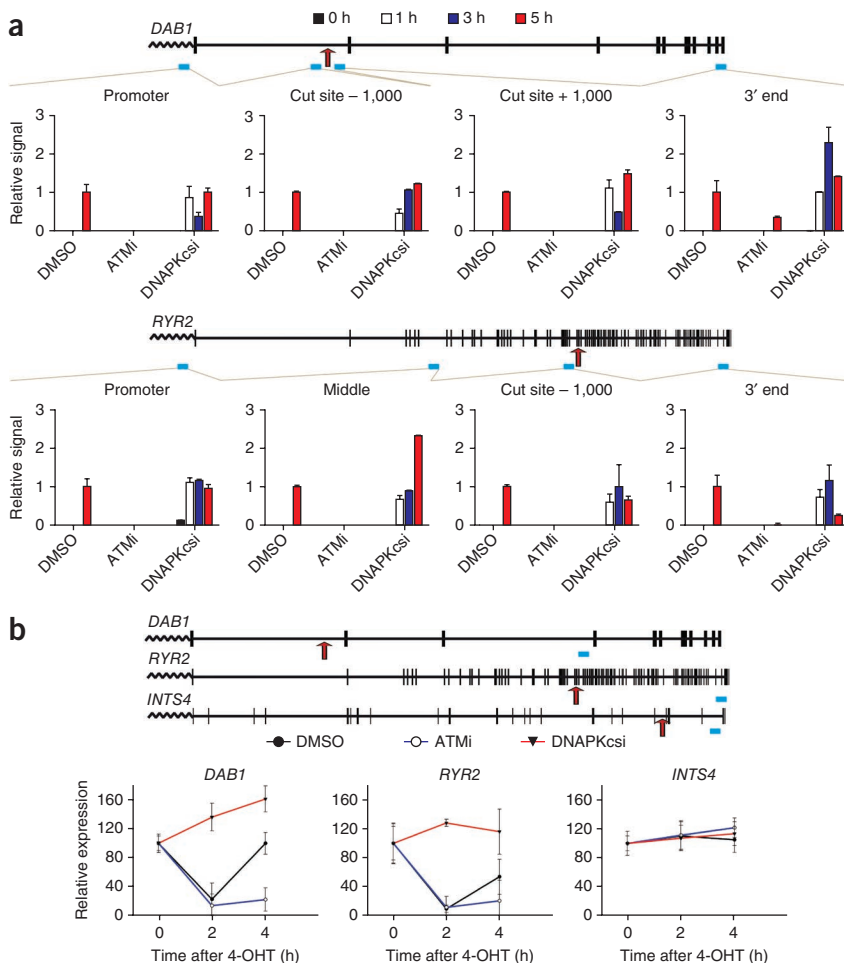
an arrest in transcription. As predicted, the occupancy of RNAPII at the promoter and the body of the *INTS4* was not altered by the addition of 4-OHT, and phosphorylation of γ-H2AX was not induced, verifying the absence of a DSB (**Fig. 5c** and **Supplementary Fig. 7c**).

To ensure that RNAPII travels on damaged chromatin when DNAPKcs is inactive, and to exclude the possibility that our observations were due to upregulation of transcription from the fraction of *DAB1* and *RYR2* genes that remained uncut in a population of cells, we carried out sequential ChIPs using RNAPII and γ-H2AX antibodies. Notably, when DNAPKcs was inhibited, RNAPII and phosphorylated H2AX overlapped early after break induction, suggesting that RNAPII processing is not affected by the spreading of the DDR signal (**Fig. 6a**). Furthermore, RNAPII coincided with γ-H2AX in the control condition 5 h after the break induction, when transcription

was gradually restored but phosphorylation of H2AX was not fully resolved (**Fig. 6a**). This observation further supports the idea that H2AX-dependent signaling does not affect RNAPII transcription.

To test whether the polymerase detected after the break was active and whether a full-length and not a truncated transcript was
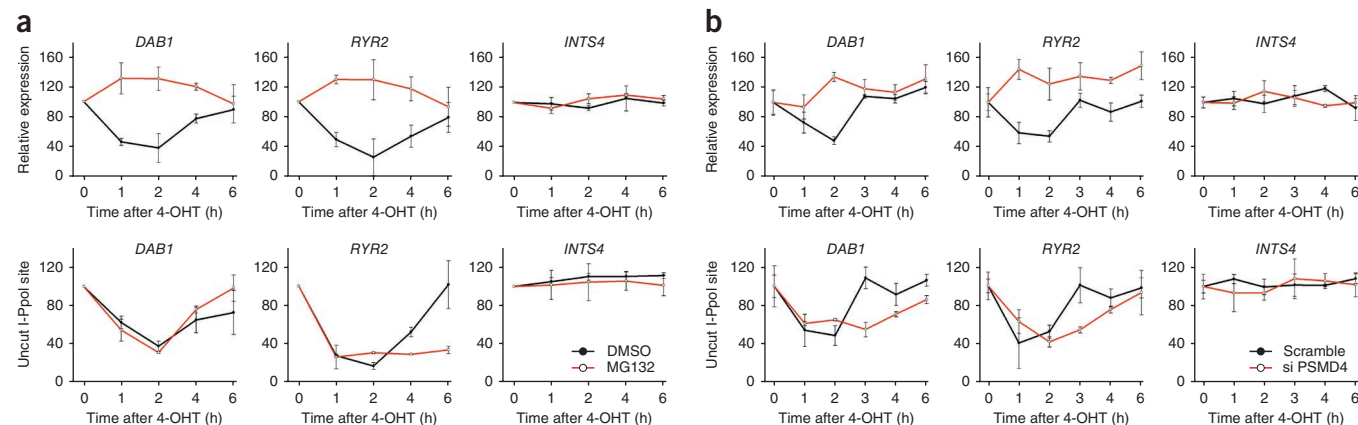

Figure 7 The proteasome is involved in transcriptional arrest after DSB induction. (**a**) Quantification of *DAB1*, *RYR2* and *INTS4* expression levels and cutting efficiencies in HeLa cells treated with DMSO and the proteasome inhibitor MG132 at 0–6 h after addition of 4-OHT. mRNA values (top) are normalized to cyclophilin B. Values for DNA content (bottom) are normalized to a part of the gene that is not affected by the break. Values represent mean ± s.d. from three independent experiments. (**b**) qRT-PCR analysis of *DAB1*, *RYR2* and *INTS4* expression levels and cutting efficiencies in HeLa cells treated with siRNA that targets a scramble sequence and PSMD4 sequence (si PSMD4) at different time points after the addition of 4-OHT. mRNA values (top) are normalized to cyclophilin B. Values for DNA content (bottom) are normalized to a part of the gene not affected by the break. Values represent mean ± s.d. from three independent experiments.

produced, we quantified nascent RNA from *DAB1* and *RYR2* under DMSO, DNAPKcs-inhibitor and ATM-inhibitor conditions. This resulted in the amplification of sequences that correspond to nascent *DAB1* and *RYR2* transcripts occurring after the I-PpoI sequence, when DNAPKcs is inhibited, which further suggests that RNAPII circumvents the break and continues transcription (**Fig. 6b**).

DSB-dependent transcription inhibition requires proteasome

To investigate whether the mechanism behind DNAPKcs-dependent RNAPII removal from RNAPII-transcribed genes after a DSB involves proteasome-dependent degradation, we monitored the *DAB1* and *RYR2* mRNA levels after 4-OHT treatment in the presence of the proteasome inhibitor MG132 (**Fig. 7a** and **Supplementary Fig. 8a**). Notably, the inhibition of the proteasome rescued the transcription defect similarly to what was observed in DNAPKcs inhibition (**Fig. 7a** and **Supplementary Fig. 8a**). It has recently been shown that the proteasome inhibitors could partially deplete ubiquitin from the cell nucleus[22]. To ensure that the effect in transcriptional rescue upon inhibition of DNAPKcs was not due to altered histone ubiquitination, we measured the levels of ubiquitination of histone H2A and the distribution of ubiquitin in the absence and presence of the DNAPKcs inhibitor (**Supplementary Fig. 8c**). We observed no reduction in ubiquitin-H2A levels upon inhibition of DNAPKcs (**Supplementary Fig. 8c**).

To test whether the effect of the proteasome inhibition on transcription of *DAB1* and *RYR2* genes after break induction is direct and not a side effect of the ubiquitin reduction following MG132 treatment, we knocked down a core subunit of the 19S proteasome complex PSMD4 that has recently been shown to be phosphorylated by ATM or ATR and to have a role in DSB repair[23–25]. Monitoring the transcription of *DAB1* and *RYR2* genes before and after break induction in these cells demonstrated that depletion of PSMD4 recapitulated the result obtained by DNAPKcs inhibition (**Fig. 7b** and **Supplementary Fig. 8b**). Downregulation of PSMD4 did not result in depletion of ubiquitin-H2A, in contrast to what was observed in the presence of MG132 (**Supplementary Fig. 8c**). Our results point to a role of the proteasome in destabilizing the RNAPII complex, leading to transcription inhibition in the presence of DSBs.

DISCUSSION

Here we report a new role for DNAPKcs in break-dependent transcriptional arrest. We also illustrate that the monoubiquitination of histone H2A is not primarily responsible for the transcription inhibition observed upon induction of a DSB at an RNAPII-transcribed gene body. Moreover, RNAPII elongation complexes do not appear to compete with the DNA-repair megacomplexes that spread across kilobases of the DSB-surrounding chromatin. Our results differ from earlier observations reporting that ATM-dependent spreading of a silencing program is involved in DSB-dependent RNAPII transcriptional inhibition[7]. We speculate that this discrepancy is due to the different numbers of breaks induced in the previous studies as well as to the topology of the breaks. Although ATM signaling might have a role in blocking transcription elongation when a large number of breaks are induced in regions proximal to a promoter of an RNAPII-transcribed gene, DNAPKcs is essential for arresting transcription when the RNAPII machinery comes across a single DSB.

Our observations suggest that it is not the break per se but DNAPKcs that presents a natural barrier to RNAPII and leads to its displacement from the surrounding chromatin. The association of DNAPKcs with DSBs is highly dynamic[18]. Previous studies have reported that impairment of the kinase activity or the phosphorylation status of DNAPKcs increases its residence time at DSB-surrounding chromatin[18]. Thus, our results,

which show that upon pharmacological inhibition of DNAPKcs, transcription is rescued and that RNAPII can circumvent a break, suggest that it is not the DNAPKcs moiety but rather its activity that is necessary for the transcriptional arrest.

We demonstrate the involvement of the proteasome complex in rescuing the transcriptional arrest induced by DSBs. In yeast, subunits of the 19S and 20S proteasome subcomplexes are recruited to DSBs through crucial repair factors and are required for efficient repair by homologous recombination and nonhomologous end-joining pathways[26]. In this study it was hypothesized that the role of the proteasome at DSBs is to degrade one or more components of the DSB-repair machinery, following the completion of repair. Although we were unable to reproducibly detect DNA damage–inducible degradation of the largest subunit of RNAPII (data not shown), our results point to a mechanism that involves DNAPKcs-dependent phosphorylation and proteasome-dependent degradation of as-yet-unidentified proteins, which leads to the dissociation of the RNAPII machinery from DSB sites.

Alternatively, one may consider the activity of proteasome components that are unrelated to protein degradation. For example, previous results have shown that depletion of PSMD4 alters the kinetics of recruitment of BRCA1 and markedly affects the recruitment of RAD51 to irradiation-induced breaks[25]. Therefore, one can speculate that PSMD4 may reinforce the recruitment of a factor that leads to destabilization of the RNAPII elongation complex.

We show here for the first time that RNAPII can bypass a DSB. This intriguing observation further supports the model in which broken chromosome ends are kept in spatial proximity[27,28]. Our findings verify earlier *in vitro* studies showing that several bacterial polymerases can efficiently transcribe over a variety of strand breaks, including gaps that are one to five base pairs in length[29–31]. Moreover, non-bulky DNA lesions, such as 8-oxoguanine, uracil and O-6-methylguanine lesions, are known to be efficiently bypassed by RNA polymerases *in vitro* and *in vivo*[32–35]. In these instances, incorporation of incorrect bases opposite the damage leads to mutant transcripts that could direct the synthesis of mutant proteins, a process termed transcriptional mutagenesis[34]. The role of DNAPKcs described here in preventing RNAPII from bypassing a DSB might be crucial in avoiding the production of mutated transcripts that could lead to cancerous phenotypes.

METHODS

Methods and any associated references are available in the online version of the paper at http://www.nature.com/nsmb/.

Note: Supplementary information is available on the Nature Structural & Molecular Biology website.

1. Jackson, S.P. & Bartek, J. The DNA-damage response in human biology and disease. *Nature* **461**, 1071–1078 (2009).
2. Kass, E.M. & Jasin, M. Collaboration and competition between DNA double-strand break repair pathways. *FEBS Lett.* **584**, 3703–3708 (2010).
3. Nyberg, K.A., Michelson, R.J., Putnam, C.W. & Weinert, T.A. Toward maintaining the genome: DNA damage and replication checkpoints. *Annu. Rev. Genet.* **36**, 617–656 (2002).
4. Somesh, B.P. *et al.* Multiple mechanisms confining RNA polymerase II ubiquitylation to polymerases undergoing transcriptional arrest. *Cell* **121**, 913–923 (2005).
5. Svejstrup, J.Q. Contending with transcriptional arrest during RNAPII transcript elongation. *Trends Biochem. Sci.* **32**, 165–171 (2007).
6. Anindya, R., Aygun, O. & Svejstrup, J.Q. Damage-induced ubiquitylation of human RNA polymerase II by the ubiquitin ligase Nedd4, but not Cockayne syndrome proteins or BRCA1. *Mol. Cell* **28**, 386–397 (2007).
7. Shanbhag, N.M., Rafalska-Metcalf, I.U., Balane-Bolivar, C., Janicki, S.M. & Greenberg, R.A. ATM-dependent chromatin changes silence transcription in cis to DNA double-strand breaks. *Cell* **141**, 970–981 (2010).
8. Kruhlak, M. *et al.* The ATM repair pathway inhibits RNA polymerase I transcription in response to chromosome breaks. *Nature* **447**, 730–734 (2007).
9. Kim, J.A., Kruhlak, M., Dotiwala, F., Nussenzweig, A. & Haber, J.E. Heterochromatin is refractory to gamma-H2AX modification in yeast and mammals. *J. Cell Biol.* **178**, 209–218 (2007).
10. Chou, D.M. *et al.* A chromatin localization screen reveals poly (ADP ribose)-regulated recruitment of the repressive polycomb and NuRD complexes to sites of DNA damage. *Proc. Natl. Acad. Sci. USA* **107**, 18475–18480 (2010).
11. Berkovich, E. Monnat, R.J. Jr. & Kastan, M.B. Roles of ATM and NBS1 in chromatin structure modulation and DNA double-strand break repair. *Nat. Cell Biol.* **9**, 683–690 (2007).
12. Shiloh, Y. ATM and related protein kinases: safeguarding genome integrity. *Nat. Rev. Cancer* **3**, 155–168 (2003).
13. Kastan, M.B. & Lim, D.S. The many substrates and functions of ATM. *Nat. Rev. Mol. Cell Biol.* **1**, 179–186 (2000).
14. Weterings, E. & Chen, D.J. DNA-dependent protein kinase in nonhomologous end joining: a lock with multiple keys? *J. Cell Biol.* **179**, 183–186 (2007).
15. Weterings, E. & Chen, D.J. The endless tale of non-homologous end-joining. *Cell Res.* **18**, 114–124 (2008).
16. Iacovoni, J.S. *et al.* High-resolution profiling of gammaH2AX around DNA double strand breaks in the mammalian genome. *EMBO J.* **29**, 1446–1457 (2010).
17. Kurimasa, A. *et al.* Requirement for the kinase activity of human DNA-dependent protein kinase catalytic subunit in DNA strand break rejoining. *Mol. Cell. Biol.* **19**, 3877–3884 (1999).
18. Uematsu, N. *et al.* Autophosphorylation of DNA-PKCS regulates its dynamics at DNA double-strand breaks. *J. Cell Biol.* **177**, 219–229 (2007).
19. Lieber, M.R. The mechanism of double-strand DNA break repair by the nonhomologous DNA end-joining pathway. *Annu. Rev. Biochem.* **79**, 181–211 (2010).
20. Sims, R.J. III, Belotserkovskaya, R. & Reinberg, D. Elongation by RNA polymerase II: the short and long of it. *Genes Dev.* **18**, 2437–2468 (2004).
21. Epshtein, V. & Nudler, E. Cooperation between RNA polymerase molecules in transcription elongation. *Science* **300**, 801–805 (2003).
22. Dantuma, N.P., Groothuis, T.A., Salomons, F.A. & Neefjes, J. A dynamic ubiquitin equilibrium couples proteasomal activity to chromatin remodeling. *J. Cell Biol.* **173**, 19–26 (2006).
23. Matsuoka, S. *et al.* ATM and ATR substrate analysis reveals extensive protein networks responsive to DNA damage. *Science* **316**, 1160–1166 (2007).
24. Słabicki, M. *et al.* A genome-scale DNA repair RNAi screen identifies SPG48 as a novel gene associated with hereditary spastic paraplegia. *PLoS Biol.* **8**, e1000408 (2010).
25. Jacquemont, C. & Taniguchi, T. Proteasome function is required for DNA damage response and fanconi anemia pathway activation. *Cancer Res.* **67**, 7395–7405 (2007).
26. Krogan, N.J. *et al.* Proteasome involvement in the repair of DNA double-strand breaks. *Mol. Cell* **16**, 1027–1034 (2004).
27. Soutoglou, E. *et al.* Positional stability of single double-strand breaks in mammalian cells. *Nat. Cell Biol.* **9**, 675–682 (2007).
28. Misteli, T. & Soutoglou, E. The emerging role of nuclear architecture in DNA repair and genome maintenance. *Nat. Rev. Mol. Cell Biol.* **10**, 243–254 (2009).
29. Zhou, W. & Doetsch, P.W. Transcription bypass or blockage at single-strand breaks on the DNA template strand: effect of different 3′ and 5′ flanking groups on the T7 RNA polymerase elongation complex. *Biochemistry* **33**, 14926–14934 (1994).
30. Zhou, W., Reines, D. & Doetsch, P.W. T7 RNA polymerase bypass of large gaps on the template strand reveals a critical role of the nontemplate strand in elongation. *Cell* **82**, 577–585 (1995).
31. Liu, J., Zhou, W. & Doetsch, P.W. RNA polymerase bypass at sites of dihydrouracil: implications for transcriptional mutagenesis. *Mol. Cell. Biol.* **15**, 6729–6735 (1995).
32. Charlet-Berguerand, N. *et al.* RNA polymerase II bypass of oxidative DNA damage is regulated by transcription elongation factors. *EMBO J.* **25**, 5481–5491 (2006).
33. Clauson, C.L., Oestreich, K.J., Austin, J.W. & Doetsch, P.W. Abasic sites and strand breaks in DNA cause transcriptional mutagenesis in *Escherichia coli*. *Proc. Natl. Acad. Sci. USA* **107**, 3657–3662 (2010).
34. Saxowsky, T.T. & Doetsch, P.W. RNA polymerase encounters with DNA damage: transcription-coupled repair or transcriptional mutagenesis? *Chem. Rev.* **106**, 474–488 (2006).
35. Saxowsky, T.T., Meadows, K.L., Klungland, A. & Doetsch, P.W. 8-Oxoguanine-mediated transcriptional mutagenesis causes Ras activation in mammalian cells. *Proc. Natl. Acad. Sci. USA* **105**, 18877–18882 (2008).

ONLINE METHODS

Cell culture. HEK293T and HeLa ER-I-PpoI stable cell lines were generated by retroviral infection of the cells with pBABE-puro-HA-ER-I-PpoI in a 6-well plate, as previously reported[36]. Twenty-four hours after the infection, the cells were plated in 150-mm dishes, and puromycin was added to a final concentration of 800 ng ml^{-1}. The surviving colonies were picked and were analyzed by immunostaining of hemagglutinin (HA)-tagged and γ-H2AX cells after 4-OHT (Sigma) treatment. The cells were grown in phenol red–free DMEM with 10% (v/v) stripped FCS buffer. The experiments were conducted in cells from the second to eighth passage after thawing. We noticed that after the ninth passage, the cells were losing the ER-I-PpoI plasmid.

To activate the nuclear translocation of ER-I-PpoI, the cells were treated with 4-OHT at 2-μM final concentration. Twelve hours before 4-OHT treatment, the medium was changed to puromycin-free medium. At the time of 4-OHT addition, the cells were kept at a maximum of 50% confluence for both cell lines. The cells were harvested at 0- to 12-h intervals after 4-OHT addition. The ATM inhibitor Ku55933 (Tocris Bioscience) and DNAPK inhibitor Nu7026 (Sigma) were used at 20-μM final concentration, and they were added 1 h prior the addition of 4-OHT. The proteosome inhibitor MG132 (Tocris Bioscience) was used at 20-μM final concentration 1 h prior to adding 4-OHT. To induce global DNA damage, the cells were treated with neocarzinostatin at a final concentration of 50 ng ml^{-1} for 15 min, washed and fixed or harvested at the indicated time points after the treatment.

Quantitative PCR and quantitative RT-PCR analysis. Total cellular RNA was purified from HeLa and HEK293T ER-I-PpoI cells using the RNeasy total RNA purification kit (Qiagen) according to the manufacturer's instructions. cDNA was synthesized with the RT-PCR kit (Qiagen) according to the manufacturer's instructions, in a final volume of 10 μl. qRT-PCR analysis was carried out using specific primers (**Supplementary Table 1**), and each reaction contained 10 ng of the total RNA template and 1 pmol of each primer. Reactions were carried out using a Roche Lightcycler 480 II system for 50 cycles. The purity of the PCR products was determined by melting curve analysis.

Premature RNA was isolated using Trizol (Molecular Research Center) according to the manufacturer's instructions. A 5-μg quantity of RNA was treated with DNase (Ambion) for 5 h and extracted with phenol-chloroform. The reverse transcription reaction was conducted using a first-strand cDNA synthesis kit (Roche) and random hexamers. The primers for quantification of the nascent transcripts are matching intronic sequences.

Genomic DNA was purified using the DNeasy blood and tissue purification kit (Qiagen) according to the manufacturer's instructions. qPCR analysis was done using specific primers (**Supplementary Table 1**), and each reaction contained 10 ng of genomic DNA template and 1 pmol of each primer in a 10-μl final volume. Reactions were carried out using a Roche Lightcycler 480 II system for 50 cycles. The purity of the PCR products was determined by melting curve analysis.

Chromatin immunoprecipitation. The ChIP analysis was done following the Dynabeads ChIP protocol from Abcam with a few modifications. Briefly, one 150-mm dish with cells that were 50% confluent was used for each time point.

The cells were cross-linked for 10 min in 0.75% (v/v) paraformaldehyde (Electron Microscopy Sciences) and then sonicated in 1% (v/v) SDS-containing sonication buffer (50 mM HEPES, pH 8, 140 mM NaCl, 1 mM EDTA, 1% (v/v) TritonX-100, 1% (v/v) SDS and a protease inhibitor cocktail (Roche). Twenty-five milligrams of chromatin were diluted ten times with RIPA buffer (50 mM Tris-HCl, pH 8, 150 mM NaCl, 1 mM EDTA, 1% Triton X-100 (v/v), 0.1% sodium deoxycholate (w/v) and 0.1% SDS (v/v)) and were used in each immunoprecipitation by adding 2 μg antibody and 30 μl (~10^7) Dynabeads M-280 (Invitrogen). The beads were washed one time for 10 min with low-salt buffer (20 mM Tris-HCl, pH 8, 150 mM NaCl, 2 mM EDTA, 1% (v/v) Triton X-100 and 0.1% (v/v) SDS), once for 10 min with high-salt buffer (20 mM Tris-HCl, pH 8, 500 mM NaCl, 2 mM EDTA, 1% (v/v) Triton X-100 and 0.1% (v/v) SDS) and once for 10 min with LiCl buffer (10 mM Tris-HCl, pH 8, 250 mM LiCl, 1 mM EDTA, 1% (v/v) NP-40 and 1% (w/v) sodium deoxycholate) and two times for 10 min each with TE buffer. The elution was done twice at 65 °C for 15 min. Cross-links were reversed by incubation at 65 °C for 6 h. The DNA was purified after proteinase K and RNaseA treatment by using phenol-chloroform extraction and was resuspended in 50 μl of TE buffer.

The signal in each experiment was calculated using the formula (immunoprecipitated sample–IgG control)/input, and each value represents a relative DNA concentration that is based on the standard curve of the input. The antibodies used are described in **Supplementary Table 1**.

For sequential ChIP experiments, complexes from the initial RNAPII ChIP experiments were eluted two times with 10 mM DTT at 37 °C for 30 min and diluted 100 times in a buffer containing 50 mM Tris, pH 8, 1 mM EDTA, 150 mM NaCl, 1% (v/v) Triton X-100, 0.1% (w/v) sodium deoxycholate, and re-immunoprecipitated with anti-γ-H2AX.

To calculate the relative signal in samples where signal was observed, we gave a value of 1 to the DMSO 5-h signal as a reference value with which the other samples were compared.

Acidic histone extraction. Acidic extraction of histones was carried out using the Abcam protocol (http://www.abcam.com/index.html?pageconfig=resource &rid=11410).

Calf intestinal phosphatase treatment. Protein samples used for calf intestinal phosphatase treatment were separated and transferred to nitrocellulose as indicated at the western blot protocol. After the electroblotting, the membranes were treated with 100 units of calf intestinal phosphatase (New England Biolabs) in 5 ml of 1× NEB3 buffer and incubated overnight for 16 h at 37 °C. After the treatment, the membranes were washed twice with PBS plus 0.1% Tween 20 and blocked for 1 h in 5% (w/v) nonfat dry milk in PBS plus 0.1% Tween 20.

Identification of the I-PpoI sites at the human genome. The I-PpoI sites were found using standard National Center for Biotechnology Information alignment methods.

36. Berkovich, E., Monnat, R.J. & Kastan, M.B. Assessment of protein dynamics and DNA repair following generation of DNA double-strand breaks at defined genomic sites. *Nat. Protoc.* **3**, 915–922 (2008).